JOURNAL OF COMPUTATIONAL PHYSICS **134,** 108–121 (1997)
ARTICLE NO. CP975676

Soliton Analysis in Complex Molecular Systems: A Zig-Zag Chain

P. L. Christiansen,* A. V. Savin,† and A. V. Zolotaryuk‡

*Institute of Mathematical Modelling, Technical University of Denmark, DK-2800 Lyngby, Denmark; †Institute for Problems of Physics and Technology, 119034 Moscow, Russia; ‡Bogolyubov Institute for Theoretical Physics, 252143 Kyiv, Ukraine
E-mail: plc@imm.dtu.dk

Received July 17, 1996; revised February 11, 1997

A simple numerical method for seeking *solitary wave* solutions of a permanent profile in molecular systems of big complexity is presented. The method is essentially based on the minimization of a finite-dimensional function which is chosen under an appropriate discretization of time derivatives in equations of motion. In the present paper, it is applied to a zig-zag chain backbone of coupled particles, each of which has *two* degrees of freedom (longitudinal and transverse). Both topological and nontopological soliton solutions are treated for this chain when it is (i) subjected to a two-dimensional periodic substrate potential or (ii) considered as an isolated object, respectively. In the first case, which may be considered as a zig-zag generalization of the Frenkel–Kontorova chain model, two types of kink solutions with different topological charges, describing vacancies of one or two atoms (I- or II-kinks) and defects with excess one or two atoms in the chain (I- or II-antikinks), have been found. The second case (isolated chain) is a generalization of the well-known Fermi–Pasta–Ulam chain model, which takes into account transverse degrees of freedom of the chain molecules. Two types of stable nontopological soliton solutions which describe either (i) a supersonic solitary wave of longitudinal stretching accompanied by transverse slendering or (ii) supersonic pulses of longitudinal compression propagating together with localized transverse thickening (bulge) have been obtained.

1. INTRODUCTION

Considerable progress has been made in understanding the wave mechanical properties of one-dimensional (1D) lattice models (see, e.g., the recent book [1] and some pioneering works such as Refs. [2–7]), including also their applications to describe the charge and energy transport in condensed matter physics [8] and biology [9–11]. However, in real physical systems, even in quasi-1D chains (e.g., biomolecules), besides the *longitudinal* direction, atoms (molecules or groups of atoms) can also move in one or two perpendicular directions and therefore the studies of chain models with transverse degrees of freedom are of great interest. Thus, it was discovered that the solitonic excitations in 1D nonlinear lattices are extremely sensitive to their transverse perturbations [12, 13] and a series of studies on soliton propagation in nonlinear lattices, when transverse motions of chain molecules are taken into account, should be mentioned [14–16]. Moreover, in some cases the transverse displacements of molecules are considered as the most important motions in biophysical processes. Thus, in the DNA molecule, the stretching of the base-pairs in the transverse direction determines the fundamental mechanism of the denaturation of this molecule. The Peyrard–Bishop model of DNA melting [17–19] has just been formulated in terms of only transverse motions of the two complementary strands. In some cases, nonlinear dynamical processes can be modelled by 1D two-sublattice models [20–23] and described by coupled lattice fields. As a rule, in these cases as well as in many other situations, it is quite difficult to treat analytically solitary wave solutions of equations of motion. Therefore, this particular type of solutions should be found by means of specific numerical methods. To this end, Eilbeck and Flesch [24] suggested a pseudo-spectral method which afterwards was developed and applied to the whole variety of nonlinear dynamical systems [25]. However, in some cases, e.g., for sufficiently smooth solitary wave solutions, it is more efficient to avoid the spectral expansions and therefore to simplify essentially the numerical procedure.

In this contribution we will deal with a numerical method of looking for solitary wave solutions in an anharmonic atomic (molecular) chain in which the particles are allowed to move in both the longitudinal and transverse directions. Such as 2D molecular chain is supposed to have some regular structure when it is found in an undistorted (ground) state. Such a requirement immediately leads with necessarity to the existence of some secondary structure and this is really the case in biology for many macromolecules (DNA, protein, etc.). Geometrically, the secondary structure is realized in the form of a helix. For simplicity, we consider in the present paper only one transverse degree of freedom. As a result, the 3D helical structure is essentially simplified, transforming into the "2D helix" which is merely a planar *zig-zag* chain. Then the primary and secondary structures are provided by the first- and second-

0021-9991/97 $25.00

neighbor intermolecular interactions, respectively. Such a system can be considered as the simplest theoretical model of an isolated molecular chain and it corresponds to the realistic situation in biomolecular sciences. In fact, the zig-zag backbone studied in the present paper is the most simple generalization of the well-known Fermi–Pasta–Ulam chain model [2] that includes transverse degrees of freedom of its particles.

It should be emphasized that the important point of the zig-zag model is the secondary structure, i.e., the second-neighbor interactions. Even in the 1D chain, the introduction of the second-neighbor interactions crucially changes the dynamics of the system [26, 27]. Therefore the zig-zag structure with the first- and second-neighbor interactions which may be referred to as valence and hydrogen bonds, respectively, essentially sophisticate the theory. Note that even if the molecules are assumed to be coupled by harmonic forces, an effective anharmonicity appears because of the geometry of the system. For breather-like solutions, the effects of such a ''geometric'' nonlinearity have previously beeen investigated by Cadet [28].

On the other hand, when this zig-zag chain is subjected to a 2D periodic (in the longitudinal direction) substrate potential, then we obtain the zig-zag generalization of the well-known Frenkel–Kontorova (FK) model [29] which was originally introduced in the theory of dislocations in solids to describe the simplest situation when a chain of atoms in crystal is assumed to contain a dislocation while its crystal environment is modelled by a periodic 1D substrate potential. One of the generalized versions of the 1D FK model which takes into account transverse degrees of freedom is the Braun–Kivshar (BK) model [30, 31]. This model has been suggested to describe the dynamics of a chain of atoms interacting via a repulsion potential and subjected to a 2D substrate potential which is periodic in the longitudinal direction and parabolic in the transverse direction. Compared to this version, we assume the 2D substrate potential to have the commensurate zig-zag relief, so that its global degenerate minima exactly coincide with the vertices of the zig-zag structure. Then a certain zig-zag-like ''channel'' appears in this 2D potential relief, along which the global minima and the barriers having a saddle form, alternate in the longitudinal direction. This modified generalization of the FK model describes the situation when quasi-1D molecule crystals are formed by parallel zig-zag molecular chains. The zig-zag substrate relief gives rise to the existence of topological soliton (kink and antikink) solutions with properties which differ from those in both the FK and BK models. At least, two types of these solutions which have differing topological charges can be treated exactly by using the numerical techniques developed in the present paper. Since the numerical method is easier for the case with substrate, we start with this system and then we improve the discretization procedure in order to apply it to an isolated zig-zag chain.

The paper is organized as follows. In Section 2, we describe the planar zig-zag model with the first- and second-neighbor interactions and construct a 2D substrate potential. In this section, we derive the basic equations of motion which have the difference-differential form. In Section 3, we find numerically two-component kink solutions that describe two types of topological defects. The kink dynamics including different collisions of the defects is also studied by numerical simulations. In Section 4, we improve the numerical method used in the previous section and find nontopological soliton solutions for an isolated zig-zag chain. The dynamics of these solitons is also studied there. Finally, a discussion in Section 5 concludes the paper.

2. A ZIG-ZAG CHAIN MODEL AND A 2D SUBSTRATE POTENTIAL

Let particles (atoms, molecules or groups of atoms) be linked together in a 2D zig-zag chain, as illustrated in Fig. 1, by the first- and second-neighbor forces with the stiffness constants K_1 and K_2, respectively. The chain backbone, with the lattice spacing l, is directed along the X axis and it can be considered as consisting of two coupled linear chains. Let the molecules of this backbone be situated at the sites $X = nl$, with the integers $n = 0, \pm 1, \ldots$ for one of these chains and with the half-integers $n = \pm\frac{1}{2}, \pm\frac{3}{2}, \ldots$ for the other chain (see Fig. 1). The molecules are allowed to move in the XY plane, so that they have two degrees of freedom, namely, the longitudinal (x_n) and transverse (y_n) displacements from the equilibrium positions, i.e., from the vertices of the regular (undistorted) zig-zag structure. As shown in Fig. 1, the dimensionless parameter h describes the geometry of the chain, namely the thickness of the zig-zag backbone (given in units of the lattice spacing l). Then the equilibrium distance between each pair of the first neighbors is determined by the dimensionless parameter $b = (h^2 + \frac{1}{4})^{1/2}$.

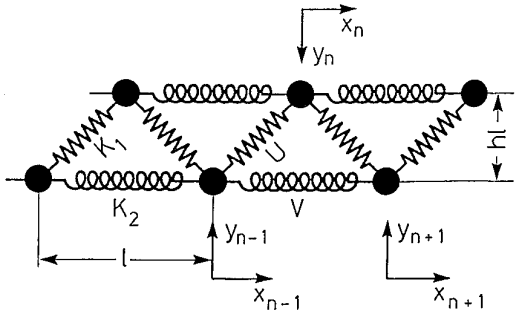

FIG. 1. Schematic representation of the zig-zag chain with $h = \frac{1}{2}$.

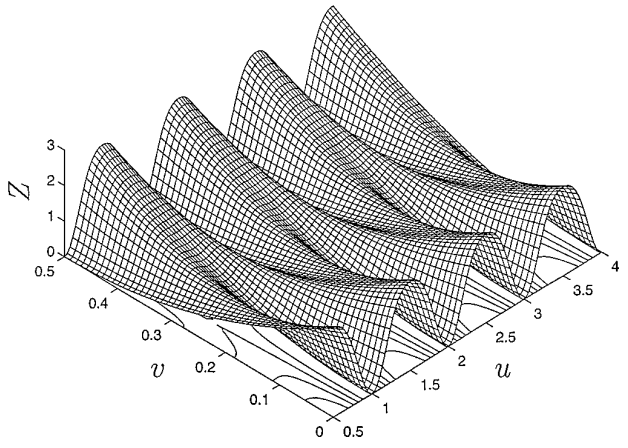

FIG. 2. The 2D potential relief given by the function (3) with $h = \frac{1}{2}$.

The described zig-zag chain is supposed to be an isolated object, on one side, and it can be subjected to a 2D on-site potential with a zig-zag relief $Z(u, v)$ shown in Fig. 2, on the other side, In the latter case, the global degenerate minima of this potential are assumed to coincide exactly with the vertices of the undistorted chain (the commensurate case). In other words, when the chain particles are situated at the vertices of the zig-zag structure, then the intermolecular bonds are undistorted and such a configuration forms one of the degenerate ground states of the system.

The 2D on-site (substrate) potential $Z(u, \mathrm{v})$ with a zig-zag relief can be constructed by using a pair of two periodic functions $\mathrm{f}(u)$ and $g(u)$ of the dimensionless longitudinal coordinate $u = X/l$ with the following properties of periodicity:

$$f(u + \tfrac{1}{2}) = f(u), \quad g(u + 1) = g(u). \tag{1}$$

Both these functions are normalized according to the inequalities $0 \le f \le 1$ and $0 \le g \le h$ and they are relatively shifted along the X axis with respect to each other in such a way that $f(\mathrm{n}/2) = 0$, $g(n) = 0$ and $f(n \pm \frac{1}{4}) = 1$, $g(n + \frac{1}{2}) = h$ for all $n = 0, \pm 1, \ldots$. In particular, for computations we use the following explicit forms:

$$f(u) = \sin^2(2\pi u), \quad g(u) = h \sin^2(\pi u). \tag{2}$$

Let $f''(n/2) = \Omega_0^2$, where Ω_0 is the dimensionless characteristic frequency of small-amplitude oscillations of the chain particles at the minima of the 2D substrate potential $Z(u, v)$ and the primes mean the differentiation. Then the potential $Z(u, v)$ with the frequency Ω_0 can be represented in the form

$$Z(u, v) = f(u) + \tfrac{1}{2}\Omega_0^2[v - g(u)]^2, \tag{3}$$

so that

$$\frac{\partial^2}{\partial u^2} Z(u, v)|_{u=0,v=0} = \frac{\partial^2}{\partial v^2} Z(u, v)|_{u=0,v=0} = \Omega_0^2, \tag{4}$$

as is required. It follows from the representation (3) that $f(u)$ and $g(u)$ may be referred to as "barrier" and "channel" functions, respectively.

The total Hamiltonian of the planar zig-zag system with the substrate potential described above is

$$H = \sum_n \left\{ \frac{1}{2} M(\dot{x}_n^2 + \dot{y}_n^2) + Kl^2[U(r_n) + V(q_n)] + \varepsilon_0 Z(u_n, v_n) \right\}, \tag{5}$$

where M is mass of the chain particles, K is the characteristic stiffness constant, and the dot denotes the differentiation with respect to time t. The dimensionless intermolecular potentials $U(r)$ and $V(q)$ describe the primary (between the nearest neighbors) and secondary (between the second neighbors) interactions, respectively. According to Fig. 1, the deviations from the equilibrium lengths are defined by

$$r_n = \left[\left(\frac{1}{2} + \frac{x_{n+1} - x_n}{l} \right)^2 + \left(h - \frac{y_n + y_{n+1}}{l} \right)^2 \right]^{1/2} - b,$$
$$q_n = \left[\left(1 + \frac{x_{n+1} - x_{n-1}}{l} \right)^2 + \left(\frac{y_{n+1} - y_{n-1}}{l} \right)^2 \right]^{1/2} - 1. \tag{6}$$

The potentials $U(r)$ and $V(q)$ are normalized by $U(0) = 0 = V(0)$ and $U''(0) = \kappa_1$, $V''(0) = \kappa_2$ with $\kappa_1 = K_1/K$, and $\kappa_2 = K_2/K$ being the dimensionless stiffness constants of the first- and second-neighbor forces, respectively. The parameter ε_0 describes the height of the barriers in the potential $Z(u, v)$.

For the dimensionless description it is convenient to introduce the normalized time τ and to rescale the spatial variable x_n and y_n as

$$\tau = (K/M)^{1/2} t, \quad u_n(\tau) = x_n(t)/\mathrm{l}, \quad v_n(\tau) = y_n(t)/l. \tag{7}$$

Then the dimensionless Lagrangian which corresponds to the Hamiltonian (5) takes the form

$$\mathscr{L} = \mathscr{L}\left\{ \frac{du_n}{d\tau}, u_n; \frac{dv_n}{d\tau}, v_n \right\}$$
$$= \sum_n \left\{ \frac{1}{2} \left[\left(\frac{du_n}{d\tau} \right)^2 + \left(\frac{dv_n}{d\tau} \right)^2 \right] - U(r_n) - V(q_n) - \nu Z(u_n, v_n) \right\}, \tag{8}$$

where $\nu = \varepsilon_0/Kl^2$. When the zig-zag chain is considered as an isolated object, then $\nu = 0$, and we put $\nu = 1$ in the case if the chain is subjected to the substrate potential $Z(u, v)$. Both of these cases will be treated separately. Since the case with > 0 is easier than the situation without the substrate ($\nu = 0$), we start with the former case.

3. THE ZIG-ZAG CHAIN IN A COMMENSURATE SUBSTRATE POTENTIAL

We consider in this section the simplest case when both of the intersite interactions $U(r)$ and $V(q)$ are given by harmonic forces. However, it should be emphasized that the chain still contains an anharmonicity due to the zig-zag geometry. This kind of anharmonicity is referred to as geometric nonlinearity. In this case, we will be dealing with topological solitons which are formed due to the presence of the substrate potential $Z(u, v)$, but not the intersite anharmonicity. The intersite anharmonicity including the geometric nonlinearity will only change some of the properties of the kinks (and antikinks) considered below. Hence, in the Hamiltonian (5) we put $U(r) = r^2/2$ and $V(q) = q^2/2$ and then the corresponding (dimensionless) Euler–Lagrange equations of motion take the form ($\nu = 1$)

$$\begin{aligned}
\frac{d^2u_n}{d\tau^2} &= \kappa_1\left[u_{n+1} - 2u_n + u_{n-1} - \left(\frac{1/2 + u_{n+1} - u_n}{1 + r_n/b} - \frac{1/2 + u_n - u_{n-1}}{1 + r_{n-1}/b}\right)\right] \\
&\quad + \kappa_2\left[u_{n+2} - 2u_n + u_{n-2} - \left(\frac{1 + u_{n+2} - u_n}{1 + q_{n+1}} - \frac{1 + u_n - u_{n-2}}{1 + q_{n-1}}\right)\right] - \frac{\partial}{\partial u_n} Z(u_n, v_n), \\
\frac{d^2v_n}{d\tau^2} &= \kappa_1\left[2h - v_{n-1} - 2v_n - v_{n+1} - \left(\frac{h - v_{n-1} - v_n}{1 + r_{n-1}/b} + \frac{h - v_n - v_{n+1}}{1 + r_n/b}\right)\right] \\
&\quad + \kappa_2\left[v_{n+2} - 2v_n + v_{n-2} - \left(\frac{v_{n+2} - v_n}{1 + q_{n+1}} - \frac{v_n - v_{n-2}}{1 + q_{n-1}}\right)\right] \\
&\quad - \frac{\partial}{\partial v_n} Z(u_n, v_n).
\end{aligned} \tag{9}$$

Below these equations will be studied numerically and in order to find their solitary wave solutions we will develop a minimization scheme. When these solutions have been found, they can be chosen as *initial* conditions for numerical simulations of the equations of motion (9). Then a *final* profile of the lattice fields $u_n(\tau)$ and $v_n(\tau)$ obtained under the simulations at sufficiently large times τ allows us to conclude whether or not the initial condition found by the minimization procedure is a stable solution of Eqs. (9).

3.1. *Discretization of the Time Derivatives*

The main point in our numerical approach is an appropriate choice of a discrete functional for a minimization procedure. Such a functional can be constructed from the corresponding Lagrangian of the system by replacing the time derivatives $du_n/d\tau$ and $dv_n/d\tau$ by appropriate spatial differences of these lattice fields. Such a replacing procedure can be applied to those lattice functions which (i) are sufficiently *smooth* from site to site and (ii) have a *stationary* profile moving with some velocity, s, so that we can write $u_n(\tau) = u(n - s\tau)$ and $v_n = v(n - s\tau)$. Clearly, in the case of standing ($s = 0$) profiles, since the time derivatives are absent, the fields u_n and v_n are not required to be smooth functions on the lattice.

For seeking topological soliton solutions which exist only in the case with the substrate potential $Z(u, v)$, it is sufficient to adopt the most simple spatial discretization as

$$\begin{aligned}
\frac{du_n}{d\tau} &= -su'(n - s\tau) \simeq -s(u_{n+1} - u_{n-1}), \\
\frac{dv_n}{d\tau} &= -sv'(n - s\tau) \simeq -s(v_{n+1} - v_{n-1}).
\end{aligned} \tag{10}$$

Note that the dimensionless distance between the $(n - 1)$th and $(n + 1)$th lattice sites is 1. Then substituting these approximate relations into the Lagrangian (8), we obtain the finite-dimensional function

$$\begin{aligned}
\mathcal{L} = \mathcal{L}(u_1, \ldots, u_N; v_1, \ldots, v_N) = \sum_{n=1}^{N}\left[\frac{1}{2}s^2(u_{n+1} - u_{n-1})^2\right. \\
\left. + \frac{1}{2}s^2(v_{n+1} - v_{n-1})^2 - \frac{1}{2}\kappa_1 r_n^2 - \frac{1}{2}\kappa_2 q_n^2 - Z(u_n, v_n)\right],
\end{aligned} \tag{11}$$

where N is the number of the chain particles. This discrete Lagrangian can be studied for extremum points, for instance, by using the steepest descent method. Obviously, the extremum conditions $\partial\mathcal{L}/\partial u_n = 0$ and $\partial\mathcal{L}/\partial v_n = 0$ immediately yield the difference equations which can be obtained from Eqs. (9) by the substitution of the second-order time derivatives, $d^2u_n/d\tau^2$ and $d^2v_n/d\tau^2$ by the second-order spatial difference derivatives $4s^2(u_{n+2} - 2u_n + u_{n-2})$ and $4s^2(v_{n+2} - 2v_n + v_{n-2})$, respectively.

3.2. *Two-Component Topological Solitons*

To find soliton solutions by minimization of the Lagrangian function (11), we need to specify appropriate bound-

ary conditions. Since the zig-zag chain is subjected to the commensurate substrate potential, we expect to obtain topological soliton (kink) solutions. We look for the solutions that have the topological charges $Q = \mp 1, \mp 2$ where the upper (lower) signs correspond to kinks (antikinks). The kink solutions describe a vacancy of one (I-kink, $Q = -1$) or two (II-kink, $Q = -2$) particles, whereas the antikink solutions correspond to excess one (I-antikink, $Q = 1$) or two (II-antikink, $Q = 2$) particles in the chain. Then the corresponding boundary conditions at the chain ends have the form

$$\begin{aligned} &u_1 = 0, u_N = 1/2, v_1 = 0, v_N = h \text{ (I-kink)}, Q = -1; \\ &u_1 = 1/2, u_N = 0, v_1 = h, v_N = 0 \text{ (I-antikink)}, Q = 1; \\ &u_1 = 0, u_N = 1, v_1 = v_N = h \text{ (II-kink)}, Q = -2; \\ &u_1 = 1, u_N = 0, v_1 = v_N = 0 \text{ (II-antikink)}, Q = 2. \end{aligned} \tag{12}$$

Now we can give the formulation of minimization problem for the function (11) as

$$\mathcal{L}(u_1, \ldots, u_N; v_1, \ldots, v_N) \to \min_{u_2, \ldots, u_{N-1}; v_1, \ldots, v_{N-1}} \tag{13}$$

with the boundary conditions (12) to be fixed under the minimization process. Since we are interested only in soliton solutions, at a given value of the velocity $s > 0$, only those points in the $2N$-dimensional space are chosen as solutions of the minimization problem which give (i) *localized* and (ii) *smooth* profiles on the lattice. Nonsmooth profiles are considered only if $s = 0$, when the approximate substitution (10) is absent and therefore the minimization (13) yields exact *standing* solutions. Therefore, for all $s > 0$ localized broad profiles obtained under the minimization process (13) can be accepted in our scheme as appropriate soliton solutions. Other profiles which contain, for instance, oscillating tails, are excluded from the further consideration.

To describe two-component profiles which are found only numerically, it is convenient to define the soliton width

$$D = 2\left[\sum_n (n - N_c)^2 (u_{n+1} - u_n)/(u_N - u_1)\right]^{1/2} \tag{14}$$

which depends on the kink velocity s and where

$$N_c = \frac{1}{2} + \sum_n \frac{u_{n+1} - u_n}{u_N - u_1} \tag{15}$$

is the center of the defect. Another quantity which is useful to describe a soliton solution is the kink energy

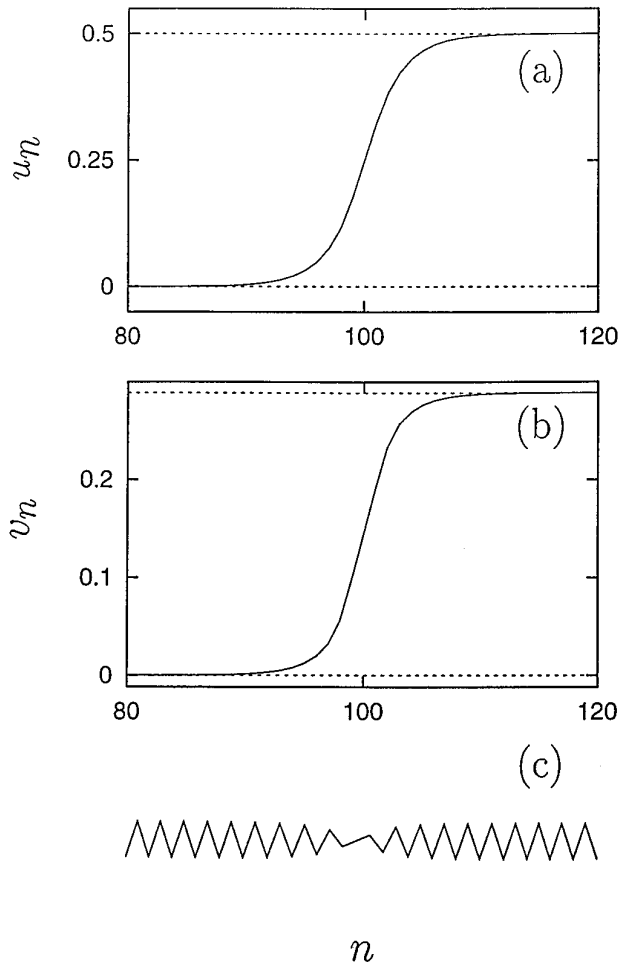

FIG. 3. The standing two-component kink ($Q = -1$) profile ($E = 9.1$ and $D = 7.0$) found by the minimization of the function (11): (a) longitudinal (u_n) displacements; (b) transverse (v_n) displacements; and (c) the corresponding deformation of the zig-zag chain.

$$\begin{aligned} E = E(s) = \sum_n \Big[&\frac{1}{2} s^2 (u_{n+1} - u_{n-1})^2 \\ &+ \frac{1}{2} s^2 (v_{n+1} - v_{n-1})^2 \\ &+ \frac{1}{2} \kappa_1 r_n^2 + \frac{1}{2} \kappa_2 q_n^2 + Z(u_n, v_n) \Big] \end{aligned} \tag{16}$$

which also depends on the velocity s. The results of the solution of the minimization problem (13) are particularly presented in Figs. 3 and 4, where the I- and II-kink profiles are plotted. At the same parameter values, the profiles describing the topological defects with the negative charges $Q = -1$ and $Q = -2$, respectively, are much broader than the profiles corresponding to the positive defects ($Q = 1$, 2). Thus, for instance, if $\kappa_1 = 1000$, $\kappa_2 = 100$ and $\Omega_0^2 = 20$,

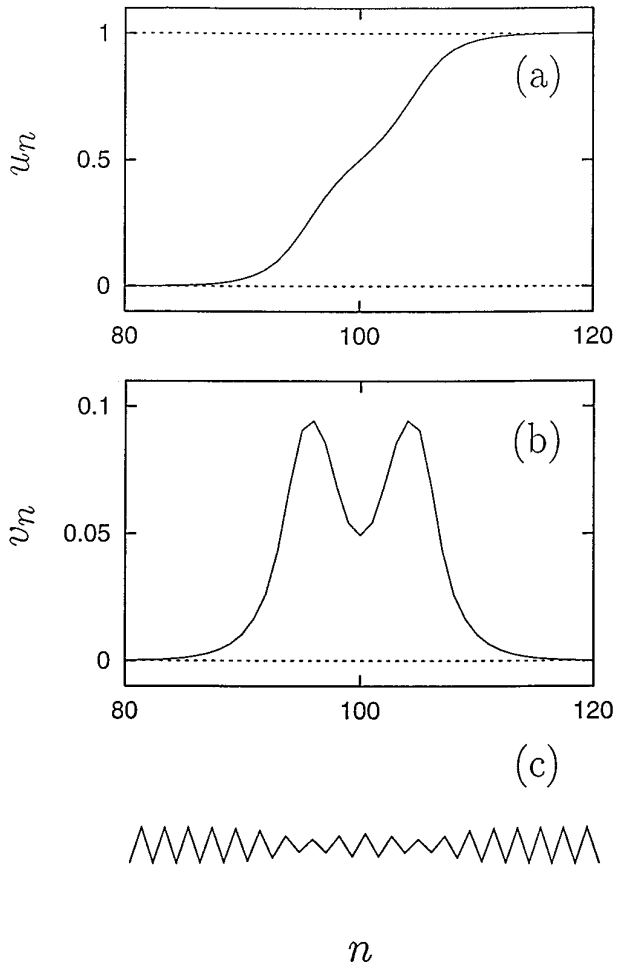

FIG. 4. The same for the standing II-kink profile with $Q = -2$ ($E = 19.8$ and $D = 11.3$).

the standing ($s = 0$) kink with the charge $Q = -1$ has the width equal to seven lattice sites ($D = 7.0$) and the kink width for $Q = -2$ is $D = 11.3$. For the antikinks with $Q = 1$, we have $D = 2.6$ while for the second type ($Q = 2$) the width is $D = 2.8$. Since the positive defects (antikinks with $Q = 1, 2$) are very narrow objects, they form the pinned states which cannot propagate freely along the chain. As for the moving kink solutions, we have found the intervals of the velocity s, for which the soliton solutions obtained by the minimization process (13) exist. Thus, we have found that the function (11) reaches its minimum only if the kink velocity belongs to the segments $0 \le s \le 0.343$ if $Q = -1$ and $0 \le s \le 2.352$ if $Q = -2$. Outside these segments, there are no minima corresponding to localized smooth profiles.

The substitution of the solutions obtained by the minimization into Eqs. (14) and (16) allows us to describe the dependence of the energy and width of both the types of kinks on their velocity s. We have examined this behavior and found that, in general, the kink width $D(s)$ is a monotonically decreasing function while the energy $E(s)$ increases with the growth of s. However, with the system parameters $\kappa_1 = 1000$, $\kappa_2 = 100$, and $\Omega_0^2 = 20$, these dependencies in the corresponding segments of admissible values of the velocity s are practically negligible. In order to get a more visible velocity dependence, we have strengthened the stiffness constants κ_1 and κ_2 and lowered the height of the substrate potential barrier. Thus, in Fig. 5 we have plotted the width dependence for the parameter values $\kappa_1 = 10000$, $\kappa_2 = 1000$, and $\Omega_0^2 = 10$. In this case, the interval of admissible velocities of the kink with the charge $Q = -2$ is longer: $0 \le s \le 6.9$. Again, as illustrated by Fig. 5, we have only broad solitons (e.g., $D = 33.6$ at $s = 5$) for all admissible velocities (even including the vicinity of the critical velocity $s = 6.9$). All these results clearly show that the absence of soliton solutions with higher velocities is not caused by the discreteness of the system. Such an *abrupt* disappearance of the kink solutions above a certain value of the velocity s can be explained by the presence of two types of interatomic couplings and by the system geometry.

Since the numerical procedure for seeking soliton solutions is based on the approximation (10) resulting in the Lagrangian function (11) and it is valid only for sufficiently broad soliton solutions, one could expect that in the case of a better spatial discretization it would be possible to treat narrower solutions. To this end, we improved the numerical scheme by taking into account the lattice discreteness. More precisely, in the approximation of the second-order time derivatives $d^2u_n/d\tau^2$ and $d^2v_n/d\tau^2$ by spatial difference derivatives (applied to the equations of motion (9)), the fourth-order derivatives $-(s^2/3)(u_{n+2} - 4u_{n+1} + 6u_n - 4u_{n-1} + u_{n-2})$ and $-(s^2/3)(v_{n+2} - 4v_{n+1} + 6v_n\, 4v_{n-1} + v_{n-2})$ were added to the second-order derivatives $4s^2(u_{n+2} - 2u_n + u_{n-2})$ and $4s^2(v_{n+2} - 2v_n + v_{n-2})$, respectively. In this way, summing all these spatial difference terms expanded up to the fourth order yields exactly the continuum terms s^2u'' and s_2v''. However, with this improved discretization, we obtained exactly the same soliton profiles as in the case of the function (11), but one should notice

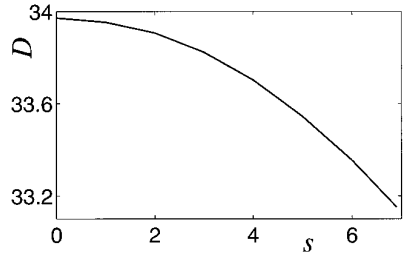

FIG. 5. Dependence of the kink width D on its velocity s for the parameter values: $\kappa_1 = 10000$; $\kappa_2 = 1000$; $\Omega_0^2 = 10$.

that these profiles (whtn they exist for $s > 0$) were always sufficiently broad. Narrow solutions were obtained only in the case of standing (pinned to the lattice) solitons and therefore in this particular case ($s = 0$), the soliton solutions are found exactly without any approximation. However, as it will be shown below in the case of an isolated chain, when very narrow solitons can propagate, such an improved discretization plays the key role in our numerical procedure.

3.3. *Dynamics of the Topological Solitons and Their Stability*

The numerical solution of the minimization problem in the case of realistic parameter values (e.g., for $\kappa_1 = 1000$ and $\kappa_2 = 100$) has shown that only the kink solutions which correspond to stretching deformation (with negative topological charge Q), as was mentioned above, have sufficiently extended profile. Using these solutions as initial conditions for simulations of the equations of motion (9), the stability of their profile and velocity has been examined. Thus, we have found that the defects with $Q = -1$ can propagate freely with velocities in the interval $0 \le s \le 0.343$. At higher velocities, the motion of any initially prepared kink-like profile, close to that from this interval, was shown to be accompanied by emission of small-amplitude waves and by gradual decreasing velocity to this value. Afterwards, the kink propagation becomes stable. The same is true for the kinks with the charge $Q = -2$. The velocity spectrum for these kinds was found to be $0 \le s \le 2.352$. Note that the emission of small-amplitude waves appears due to the nonexistence of the kink solutions outside the interval of admissible velocities.

The results of the minimization procedure have also proved that the energy of a II-kink exceeds the energy of two I-kinks, i.e., $E_{-2} > 2E_{-1}$ (according to Eq. (16)). Therefore a pair of I-kinks should be a more favorable state than the corresponding II-kink state with the same velocity s. However, the simulations of the dynamical equations (9) have shown that the II-kink is stable and it does not decay into two separate I-kinks. On the other hand, for the positive defects (antikinks with $Q = 1, 2$) which are narrow and pinned states, the situation is opposite. In this case, $E_{+2} < 2E_{+1}$ and therefore the defect with $Q = 2$ is more energetically favorable than two separate defects with $Q = 1$.

We have performed a series of numerical experiments on head-in collisions between both the types of topological defects. Some of these results are presented in Figs. 6–8. Thus, Fig. 6 demonstrates the elastic interaction of the I-kinks (vacancies) of the same topological charge $Q = -1$ and Fig. 7 illustrates the interaction between the II-kinks of the same charge $Q = 2$. The elastic collision between the negative I- and II-defects is shown in Fig. 8. The dynamical

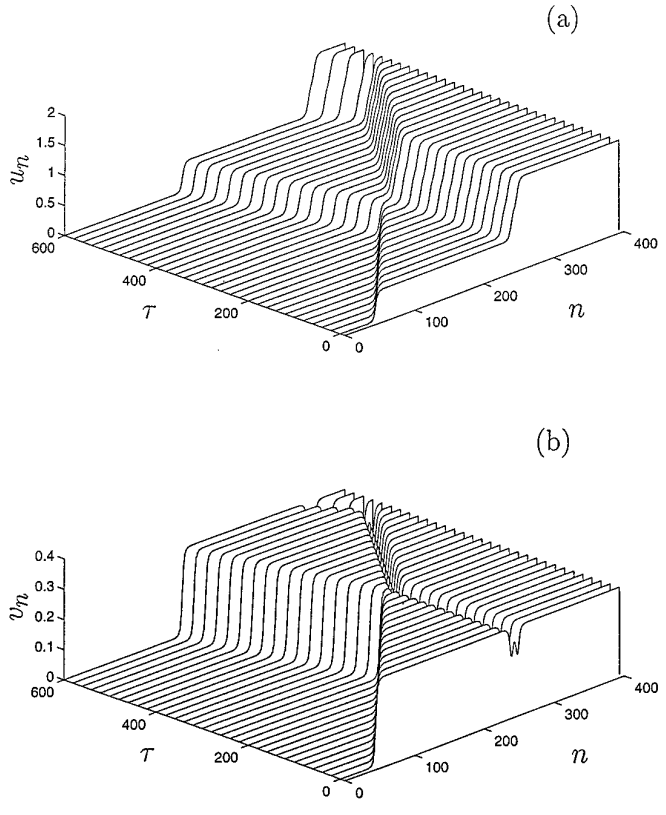

FIG. 6. Elastic collision of the moving ($s = 0.343$) defect with $Q = -1$ (I-kink) with the standing defect with $Q = -2$ (II-kink).

processes of recharging and annihilation of defects with differing topological charges have also been studied. For instance, the dynamics of creation of the defects with the charges $Q = \mp 1$ (I-kink and I-antikink) as a result of head-in collisions of the positive and negative defects with different charges Q has been observed.

4. THE ZIG-ZAG CHAIN ISOLATED

As was mentioned above, the case $\nu = 0$ corresponds to the situation when the zig-zag chain is considered as an isolated object. In this case, the existence of nontopological solitons is expected due to intersite anharmonicity. Therefore, in this section, the functions $U(r)$ and $V(q)$ should be considered of a general form. It follows from the form of the deviations r_n and q_n defined by Eqs. (6) that the dynamical equations which correspond to the Hamiltonian (5) or to the Lagrangian (8) can be rewritten in terms of the new lattice fields

$$\rho_n = u_{n+1} - u_n, \quad \eta_n = v_n + v_{n+1}. \tag{17}$$

Indeed, keeping the same notations for the deviations $r_n(\tau)$ and $q_n(\tau)$ defined as functions of τ, we have

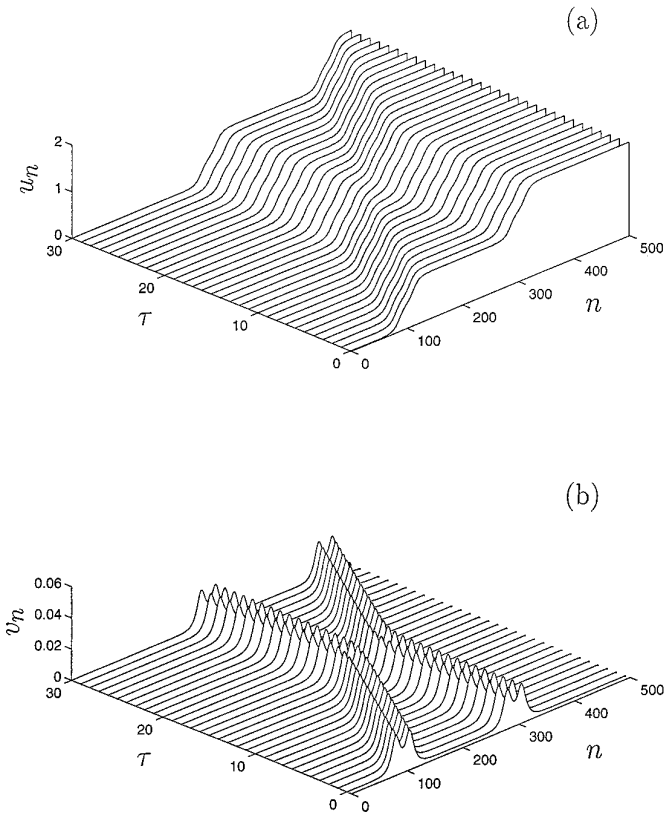

FIG. 7. Elastic reflection of the moving defect with $Q = -2$ (II-kink) from the standing defect of the same charge (II-kink).

$$r_n = \sqrt{(\tfrac{1}{2} + \rho_n)^2 + (h - \eta_n)^2} - b,$$
$$q_n = \sqrt{(1 + \rho_{n-1} + \rho_n)^2 + (\eta_n - \eta_{n-1})^2} - 1. \tag{18}$$

Then the equations of motion, which correspond to the Lagrangian (8) with $\nu = 0$, take the form

$$\frac{d^2\rho_n}{d\tau^2} = P_{n+1} - 2P_n + P_{n-1} + Q_{n+2} - Q_{n+1} - Q_n + Q_{n-1}, \tag{19}$$

$$\frac{d^2\eta_n}{d\tau^2} = -(S_{n-1} + 2S_n + S_{n+1}) + T_{n+1} - T_{n-1} + T_{n+2} - T_n, \tag{20}$$

where the abbreviations

$$P_n = \frac{\partial}{\partial\rho_n} U(r_n), \quad Q_n = \frac{\partial}{\partial\rho_n} V(q_n),$$
$$S_n = \frac{\partial}{\partial\eta_n} U(r_n), \quad T_n = \frac{\partial}{\partial\eta_n} V(q_n) \tag{21}$$

have been introduced. Such a canonical representation of the equations of motion is convenient for numerical studies of localized solutions for which the relative displacement field $\rho_n(\tau)$ very fast decreases to zero at infinity.

4.1. *The Discretization Scheme Improved*

To find *nontopological* soliton solutions, the formation of which is due to the lattice discreteness effects, we need to improve the numerical scheme used in the previous section for seeking *topological* soliton solutions. For this purpose, the approximation defined by Eqs. (10) is too crude because it does not take into account the effects of the lattice dispersion of longuitudinal waves. In order to improve the discretization version of the second time derivative in Eq. (19), the approximation of the function $\rho''(n - s\tau)$ has to contain also the fourth-order spatial derivative with an appropriate coefficient chosen in such a way that fourth-order derivative terms vanish in the continuum limit. More precisely, we write this improved discretization version as

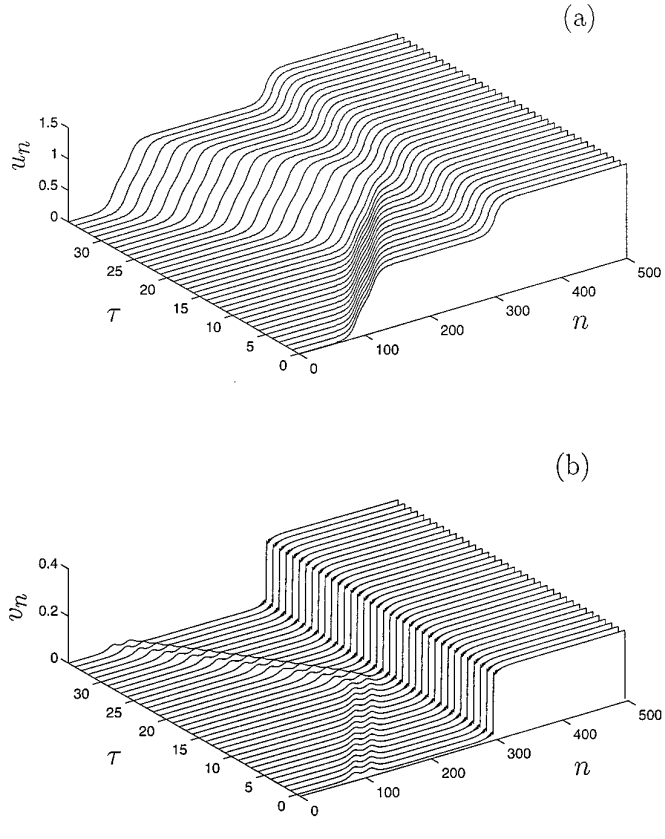

FIG. 8. Elastic reflection of the moving ($s = 0.5$) defect with charge $Q = -2$ from the pinned defect with charge $Q = -1$.

$$\frac{d^2\rho_n}{d\tau^2} \simeq 4s^2[\rho_{n+1} - 2\rho_n + \rho_{n-1} - c(\rho_{n+2} - 4\rho_{n+1} + 6\rho_n - 4\rho_{n-1} + \rho_{n-2})], \tag{22}$$

where the constant c is to be determined from the condition that the r.h.s. of this equation has to be equal to $s^2\rho''$ if all its terms are expanded to include the fourth-order terms. In other words, the last group of terms in Eq. (22) which is the fourth-order difference derivative has been introduced to cancel the corresponding fourth-order continuum derivative appearing from the first group in Eq. (22). As a result, we find $c = \frac{1}{12}$ and therefore the set of Eqs. (19) and (20) is replaced by the difference equations

$$4s^2[\rho_{n+1} - 2\rho_n + \rho_{n-1} - \tfrac{1}{12}(\rho_{n+2} - 4\rho_{n+1} + 6\rho_n - 4\rho_{n-1} + \rho_{n-2})] = P_{n+1} - 2P_n + P_{n-1} + Q_{n+2} - Q_{n+1} - Q_n + Q_{n-1}, \tag{23}$$

$$4s^2(\eta_{n+1} - 2\eta_n + \eta_{n-1}) = -(S_{n-1} + 2S_n + S_{n+1}) + T_{n+1} - T_{n-1} + T_{n+2} - T_n. \tag{24}$$

Notice that the last equation could also be discretized in the same way as Eq. (23) in order to take into account the lattice dispersion of transverse vibrations. However, this dispersion is not responsible for the formation of solitons and therefore it is not necessary to use this more complicated discretized version. In fact, we have compared the results of the minimization with both the second- and fourth-order discrete approximations of the function $v(n - s\tau)$, based on Eq. (24) and its fourth-order analogous equation, respectively, and we did not find any difference, whereas the presence of the forth-order difference term in the l.h.s. of Eq. (23) is crucial.

The difference equations (23) and (24) can be integrated and transformed to

$$\begin{aligned} s^2(\rho_{n-1} - 14\rho_{n+1} + \rho_{n+1})/3 + P_n + Q_n + Q_{n+1} = 0, \\ 4s^2(v_{n+1} - 2v_n + v_{n-1}) + S_{n-1} + S_n + T_{n-1} - T_{n+1} = 0. \end{aligned} \tag{25}$$

These equations correspond to the Lagrangian function

$$\mathscr{L} = \mathscr{L}\{\rho_n, v_n\} = \sum_n \{2s^2[\rho_n^2 + \tfrac{1}{12}(\rho_{n+1} - \rho_n)^2 + (v_{n+1} - v_n)^2] - U(r_n) - V(q_n)\}. \tag{26}$$

The extremum conditions $\partial\mathscr{L}/\partial\rho_n = 0$ and $\partial\mathscr{L}/\partial v_n = 0$ give immediately the system of the difference equations (25). However, the extremum points of the Lagrangian function (26), which correspond to soliton solutions, are not necessary to be minima or maxima. They might be saddle points as well. For instance, for the 1D Boussinesq equation, there are neither minimum nor maximum points at the corresponding Lagrangian surface. In this case, the extremum points, which correspond to the supersonic soliton solutions, are only of the saddle-type, and therefore, it is impossible to find any supersonic solution by minimization of the function (26). However, in this case we can implement a reflection of the Lagrangian surface in such a way that saddle points are transformed into minimum points at this deformed surface. The most direct and simple way is to construct the new functional

$$\mathscr{F} = \mathscr{F}\{\rho_n, v_n\} = \frac{1}{2}\sum_n \left[\left(\frac{\partial\mathscr{L}}{\partial\rho_n}\right)^2 + \left(\frac{\partial\mathscr{L}}{\partial v_n}\right)^2\right] \tag{27}$$

and then to study it for minima. Those minima which correspond to bell-shaped profiles are chosen as appropriate solitary wave solutions of our problem. Other minima describing bell-shaped configurations accompanied by any ripples, etc., are excluded from the further consideration.

4.2. *Two-Component Nontopological Solitons and Their Stability*

The presence of an interparticle anharmonicity in a standard isolated 1D chain is a necessary condition for the existence of solitons. For simplicity, we restrict ourselves here by a cubic anharmonicity. Hence, the potentials $U(r)$ and $V(q)$ are chosen in the following simplest form:

$$\begin{aligned} U(r) &= \kappa_1\left(\frac{1}{2}r^2 - \frac{\alpha}{3}r^3\right), \\ V(q) &= \kappa_2\left(\frac{2}{2}r^2 - \frac{\beta}{3}r^3\right), \quad \alpha \geq 0, \beta \geq 0. \end{aligned} \tag{28}$$

We refer to the constants α and β as to the parameters of the intrinsic anharmonicity.

We have numerically studied the zig-zag system in both cases: (i) without any intrinsic anharmonicity, when the molecules are assumed to be coupled harmonically ($\alpha = \beta = 0$), and (ii) with this type of anharmonicity, when, at least, the parameter β is positive. In the former case, we have chosen the zig-zag geometry with $h = 0.1$ by taking $\kappa_1 = \kappa_2 = 1$. The numerical minimization of the function (27) has shown that the system has a soliton solution which corresponds to localized *stretching* deformation of the chain. This solution has been proved to exist only at one value of the velocity $s = s_1 = 1.10259$. We refer to this solitary wave solution as to the stretching soliton. As is well known, there are no stable localized solutions describing stretching deformations in a 1D anharmonic chain. However, the cases of preferential (distinguished) single values for the soliton velocity are known for other nonlinear systems. Thus, Peyrard and Kruskal [7] have found a distin-

guished velocity for the propagation of the 4π-kink in the 1D discrete FK lattice. The existence of this single value is explained by the resonance interaction of two 2π-kinks from which the 4π-kink is actually formed. In the presence of the Peierls–Nabarro relief, such as interaction can be realized. In our case, the chain is isolated and the existence of the preferential velocity s_1 is caused by the specific geometry of the system. Indeed, for this solution the amplitude of the transverse displacements *exceeds* the zig-zag thickness h, so that in the vicinity of the soliton center, the upper and lower chains of the zig-zag backbone become rearranged. In other words, the chains "pass" through each other at the soliton center. As a result, the longitudinal displacements appear to be under the topological restrictions caused by such an "overslendering" of the transverse displacements, resulting in both the stretching of the longitudinal displacements and the appearance of the single value of the velocity $s = s_1$. The minima at other values of the velocity $s \neq s_1$ do not provide pure bell-shaped soliton profiles; as a rule, they give profiles with ripples. The accuracy of the solution was reached up to 10^{-10}.

The dynamics of the soliton solutions has been studied numerically in the zig-zag chain consisting of $N = 300$ molecules, with the free ends. The accuracy of integration of Eqs. (19) and (20) was estimated through the conservation of the total energy of the system. Initially, the soliton was situated at the site $n = 100$. After the passage of 100 sites, the fields $\rho_n(\tau)$ and $\eta_n(\tau)$ were replaced by $\rho_{n-100}(\tau)$ and $\eta_{n-100}(\tau)$, respectively. The similar substitution was also accomplished with the time derivatives of these fields. This procedure allows us to cut off nonsoliton contributions appearing due to emission of small-amplitude waves. These waves show up because the initial profiles obtained by the minimization procedure are only approximate, especially when they are narrow.

The numerical simulation of the equations of motion (19) and (20) has proved the stability the stretching soliton. Thus, it was shown that starting with the initial velocity $s = s_1$, the soliton propagation with the final velocity $s = s_2 = 1.10257$ was extremely stable as illustrated by Fig. 9. Thus, after the soliton passed 100000 lattice sites, during the time $\tau = 45348.8$, its velocity $s = s_2$ and two-component profile (plotted in Fig. 9 by the solid lines) were not changed. As illustrated in this figure, the initial profile found by the minimization scheme completely coincides with the final profile obtained as a result of the numerical simulation of Eqs. (19) and (20). For other velocities $s \neq s_2$, either the soliton motion is stabilized with the velocity $s = s_2$ leaving small-amplitude ripples or the soliton decays into a subsonic wave packet. Thus, the soliton propagation, which starts with any velocity $s > s_2$ is accompanied by emission of small-amplitude waves and its velocity decreases approaching the value $s = s_2$. At velocities $s < s_2$, the soliton motion is also accompanied by emission of small-amplitude waves which results in gradual breaking and final destroying the soliton.

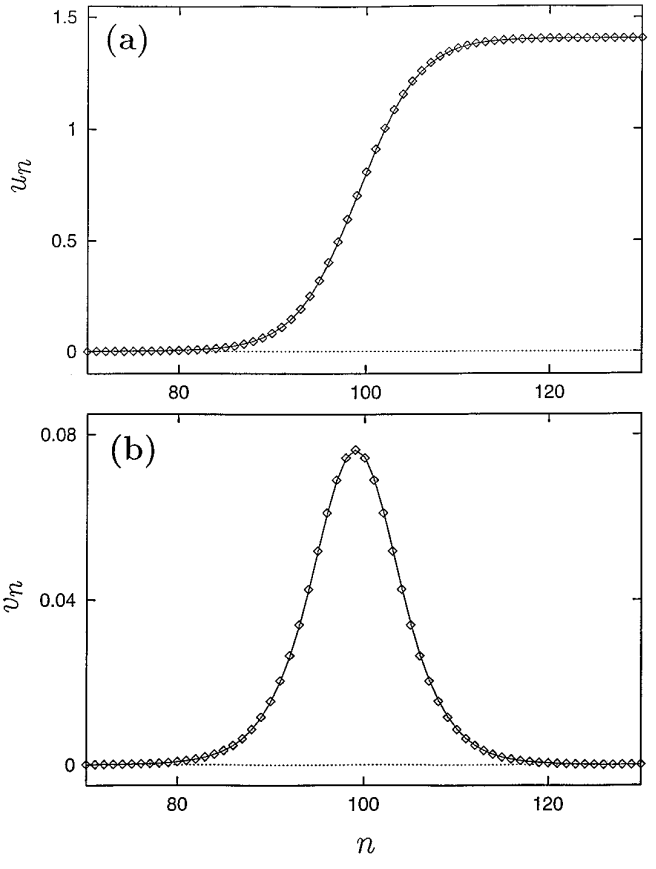

FIG. 9. The two-component soliton profiles described by the longitudinal (u_n) and transverse (v_n) displacements in the case of stretchng deformation of the isolated chain with the parameter values $h = 0.1$, $\kappa_1 = \kappa_2 = 1$, and $\alpha = \beta = 0$. The initial profile (at $\tau = 0$) has been found by the minimization of the function (27) and it is represented by squares. The final profile (solid lines) is a result of the time evolution of this profile when the soliton has passed 100000 chain sites (at $\tau = 45348.8$).

The effects of interaction of the stretching solitons have also been investigated by numerical simulations. To this end, we have simulated their head-on collision. This collision leads to the appearance of transverse vibrations of the chain molecules. The results of these simulations show that the stretching solitons are sensitive with respect to their mutual collisions resulting in the emission of transverse oscillations.

The minimization procedure has proved the existence of the second type of soliton solutions which describes a localized longitudinal *compression* of the zig-zag chain. These solutions are of the conventional type that are well known in a 1D anharmonic chain. However, in the case of the zig-zag backbone, this type of solitons can exist only in case the longitudinal anharmonicity (given by the parameter β) is sufficiently strong. In order to find these

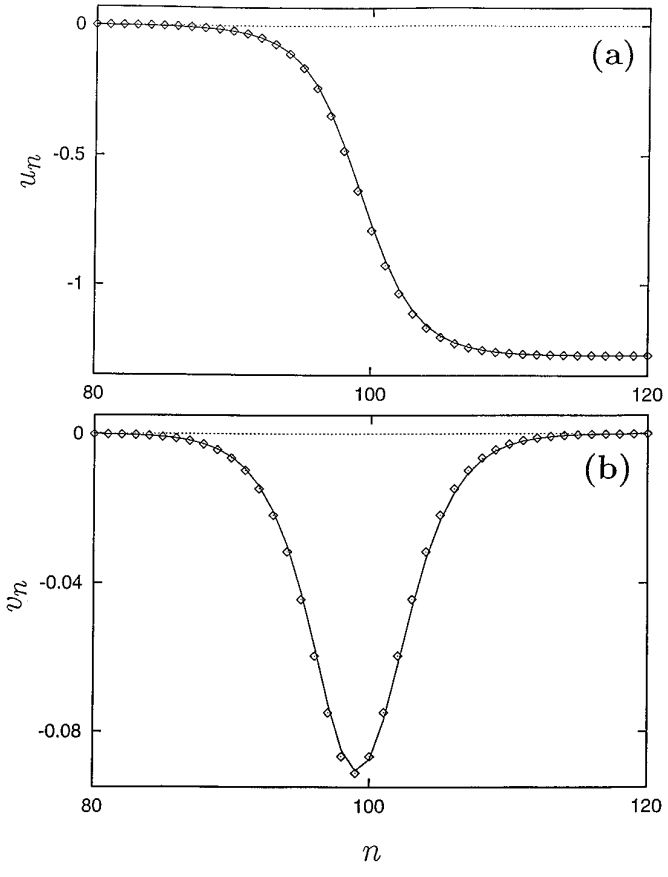

FIG. 10. The two-component profiles of the compression soliton represented by the displacement fields $u_n(\tau)$ and $v_n(\tau)$. The initial profile (shown by squares) at $\tau = 0$ has been found by the minimization procedure while the final profile (solid lines) has been obtained as a result of the time evolution of the initial profile when the soliton has passed 100000 chain sites (at $\tau = 143826.8$). The final soliton velocity is $s = 1.0993 s_0$. The chain parameters are $h = 1/2\sqrt{3}$, $\kappa_1 = 1$ and $\kappa_2 = 0.1$, $\alpha = 0$ and $\beta = 0.1$.

solutions numerically, we consider the most typical situation for molecular chains when the ratio κ_1/κ_2 is of one order. For instance, in an alpha-helix protein the constant κ_1 corresponds to hard deformations of the valence bonds while the other constant κ_2 determines the soft vibrations of the hydrogen bonds. Therefore, it is reasonable to consider the anharmonicity only in the soft bonds because they can have large amplitudes of the chain deformation. Thus, we take $\alpha = 0$, $\beta > 0$, $\kappa_1 = 1$, $\kappa_2 = 0.1$, and $h = 1/2\sqrt{3}$ (corresponding to the zig-zag angle 120°). Next, the following three values of the parameter β were chosen for numerical studies: $\beta = 0.1$, $\beta = 0.01$, and $\beta = 0.001$. The compression soliton solutions of the minimization problem were shown to exist only in the former two cases. The value $\beta = 0.001$ is too small for the existence of this type of soliton solutions. However, the stretching soliton does exist at this value. The typical two-component profile of the compression soliton is presented in Fig. 10. As demonstrated here, in the region of the soliton, the longitudinal compression and the transverse thickening take place.

Contrary to a 1D anharmonic chain, the velocity spectrum of the compression solitons in a zig-zag chain consists of a narrow band in the supersonic region which turns out to be bounded above. Thus, we have obtained the following velocity bands: $1 < s/s_0 < 1.16$ if $\beta = 0.1$ and $1 < \beta\ s/s_0 < 1.03$ if $\beta = 0.01$. Here $s_0 = \sqrt{\kappa_2}$ is the velocity of the longitudinal sound. Next, the numerical simulations have also shown that the compression solitons are dynamically stable for the anharmonicity parameter $\beta = 0.1$. Thus, at the initial velocity $s = 1.1 s_0$ the soliton propagates along 100000 chain sites during the period $\tau = 143826.8$. The soliton was moving with the final velocity $s = 1.0993 s_0$ retaining its profile. The solitons of this type have been proved to interact elastically, as demonstrated by Fig. 11.

Thus, the numerical studies have proved that in an anharmonic zig-zag chain the existence of the compression solitons depends on the magnitude of the anharmonicity parameter. For each zig-zag chain there exists a threshold value of this parameter, beginning from which the compression solitons can exist. The solitons of this type have always a finite interval of supersonic velocities. This band

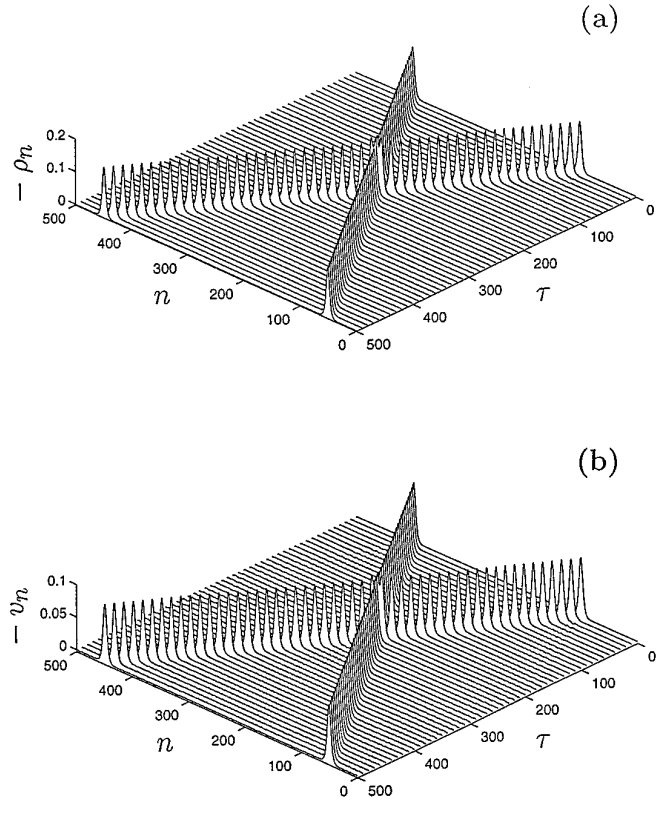

FIG. 11. Elastic head-in colission of the two compression solitons moving with velocity $s = 1.1 s_0$ in the chain with the same parameters.

enlarges with increasing the anharmonicity parameter β. The solitons loose their dynamical stability at the upper edge of the band. Sufficiently below this value, the compression solitons are dynamically stable and they interact as elastic particles.

5. DISCUSSION AND CONCLUSIONS

The suggested numerical method for looking for solitary wave solutions of stationary profile in discrete systems is based on the simple idea: as a permanent profile is assumed, the solution $\mathbf{u}_n(\tau)$ has to be of the form $\mathbf{u}(n - s\tau)$, so that $d\mathbf{u}_n/d\tau = -s\mathbf{u}'(n = s\tau)$, and then the latter (spatial) derivative is discretized appropriately, depending on what kind (topological or nontopological) of solitary wave solutions is expected to exist. Thus, to find subsonic topological soliton solutions, it is sufficient to accomplish the spatial discretization in equations of motion up to *second* order, while to get nontopological lattice solitons, formed by the counterbalance of the dispersion owing to the lattice discreteness and anharmonic interatomic (intermolecular) forces, it is necessary to involve the discretization scheme also in terms of the *fourth* order, chosen appropriately. The numerical procedure of finding extremum points corresponding to soliton solutions is also chosen depending on what kind of solutions is expected. Thus, to obtain a topological soliton profile (in general, multicomponent), it is sufficient to carry out the minimization of the corresponding discretized Lagrangian while in the case of the nontopological lattice solitons, it is necessary to transform the Lagrangian surface in such a way that its saddle points would become minimum points.

The proposed method allows us to seek only broad soliton profiles because the spatial discretization of continuous time derivatives requires a smooth dependence of solutions on the lattice site number. The method gives reliable results if the width of solitary wave solutions exceeds 4–5 lattice sites. In the class of smooth functions, one can find *all* soliton solutions and give the unique answer if they do not exist at all. Thus, for instance, in our example of the isolated zig-zag backbone, the existence of the soliton with stretching longitudinal deformation has been observed only with a *single* value of the soliton velocity. In the other case of the zig-zag backbone subjected to the periodic substrate, we have found a continuous subsonic spectrum (band) of admissible velocities of the topological soliton. Clearly, the method cannot give any indication on the reason for the absence of soliton solutions and some physical considerations might be useful.

In the case of narrow soliton solutions, the discrete spatial discretization leads to big errors and for this class of solutions the pseudo-spectral method, suggested by Eilbeck and Flesch [24] and further developed in Ref. [25], to look for soliton solutions, should be applied. The main idea of this method is the representation of a solution in the form of a finite Fourier series, its substitution into the equations of motion, and then obtaining a set of nonlinear equations with respect to the Fourier coefficients to be solved numerically. Clearly, in this approach, the discreteness of a solution (i.e., its small width) is no more an obstacle to get it (the narrower the soliton the longer the Fourier series that should be taken). Of course, broad solutions can also be obtained by the pseudo-spectral method. However, its numerical realization results in cumbersome calculations and, therefore, its applicability is justified to rather simple models for finding narrow solutions. In our case, the simplicity of the steepest-descent procedure makes it possible to be applied for numerical studies of the nonlinear dynamics of molecular systems with complex 3D structure. Therefore, one can conclude that both the minimization and pseudo-spectral methods are complementary to each other.

As for the physical examples chosen in this paper for the applications of the minimization method, one should emphasize that it was an attractive point of view to study transport processes in biopolymers on the basis of 1D nonlinear lattice models with nearest-neighbor intermolecular interactions which admit propagation of extremely stable supersonic pulses of longitudinal lattice compression. Thus, Yomosa [32] essentially applied the Fermi–Pasta–Ulam model [2] for studies of energy transport in protein. However, in general, a biopolymer should be considered as a 3D object and, therefore, its dynamics has to include also transverse degrees of freedom of the chain molecules, as was suggested, for instance, in Refs. [12–16]. On the other hand, when (i) the chain molecules are allowed to move in transverse directions and (ii) all of the intermolecular forces in the chain are assumed to have the spherical symmetry, then some additional intermolecular forces, including the next or more remote neighbors forming a secondary structure, have to be taken into account in order to stabilize a regular configuration of the chain in 3D space. In the simplest case, such a configuration has naturally the form of a so-called 3_{10}-helix [12].

In this paper, we have simplified the helical structure as much as possible by keeping the main features of the secondary structure. More precisely, the simplification has been accomplished by (i) reducing one transverse coordinate and (ii) taking into account (besides the nearest neighbors) only the second-neighbor intermolecular interactions. Such an oversimplified ''planar helix'' is nothing more than a 2D zig-zag chain in which the first- and second-neighbor molecules are coupled by intermolecular interactions. On the other hand, if such a planar chain is subjected to a commensurate 2D substrate potential, the minima of which coincide with the vertices of the zig-zag backbone, then we obtain a modified version of the Braun–Kivshar generalization [30] of the 1D Frenkel–Kontorova model

[29]. Compared to the BK chain model, which seems to be more specific with possible applications to the dynamics of adsorbed atoms on crystal surfaces (due to the presence of only a repulsive interparticle interaction), our generalization of the FK model is more straightforward. Indeed, when our 2D zig-zag chain is isolated from the planar substrate, it still has a stable ground state, similar to the 1D FK chain, because both attractive and repulsive forces are involved in the interparticle interactions.

In order to find and treat pure two-component solitary wave solutions, we have developed in the present paper a simple numerical scheme for both cases: $\nu = 0$ (isolated chain) and $\nu > 0$ (subjected to a periodic substrate). As should be expected, the existence of transverse degrees of freedom changes drastically the dynamics of the corresponding 1D chains. Thus, for the same parameter values, the vacancy defects of both types (I- and II-kinks) have been shown to exist as sufficiently extended (broad) objects which are able to propagate freely along the chain while the defects with excess particles in the chain (I- and II-antikinks) are proved to be narrow and, therefore, their pinning to the chain takes place. This kind of ''kink–antikink asymmetry'' is due to the presence of the geometric anharmonicity in the intersite coupling that exists even if both the first- and second-neighbor interactions are of the harmonic type.

The case $\nu = 0$ (isolated chain) appears to be more complicated to treat soliton solutions than the case $\nu > 0$. Compared to the standard 1D anharmonic chain, where the *compression* solitons can propagate with any supersonic velocity, the corresponding two-component solitons (longitudinal compression accompanied by transverse thickening, see Fig. 10) in the zig-zag chain actually have a narrow band of supersonic velocities. The existence of the upper bound in the velocity spectrum follows from the geometry of the zig-zag system. The solitons of this type were proved to collide elastically, as shown by Fig. 11, if their velocities are close to the lower edge of the velocity band. On the contrary, if they propagate with velocities in the vicinity of the upper edge, their collision happens to be inelastic.

The next important and new observation in our studies of the dynamics of an isolated zig-zag chain is that the stability properties of the compression solitons essentially depend on both (i) the zig-zag geometry defined by its thickness h and (ii) the magnitude of the intrinsic anharmonicity of the second-neighbor intermolecular forces (i.e., the parameter β). We have shown that the solitons with longitudinal compression cannot exist in the zig-zag chain with (i) small thickness h or (ii) week anharmonicity β, including also the case $\beta = 0$, while in a 1D chain they exist with any positive value of the anharmonicity β. The absence of a soliton solutions in this region of the parameters h and β is due to the transverse instabilities of the soliton motion which have previously been discovered in Refs. [13, 16]. However, instead of this type of solitons (localized longitudinal compression), a new stable soliton solution which corresponds to longitudinal *stretching* and transverse *slendering* (illustrated by Fig. 9) has been found numerically by using minimization techniques. This soliton solution appears due to the geometric anharmonicity and it exists for thin chains with week intrinsic anharmonicities including also the case $\alpha = \beta = 0$. However, it should be noticed that the soliton amplitude of the transverse displacements, which are directed inside the zig-zag backbone, exceeds its thickness h. As a result of such transverse ''overslendering,'' the transverse component of the soliton profile has two nodes with a bulge between them where the overslendering occurs. The second interesting feature of this soliton solution is that there exists only *one* fixed velocity at which its stable propagation happens. This value of the soliton velocity has been found numerically.

ACKNOWLEDGMENTS

This work was partially carried out with the financial support from the European Economic Community (EEC) under the INTAS Grant 94-3754. Both of us (A.V.S. and A.V.Z.) also are grateful to the MIDIT Center and the Institute of Mathematical Modelling of the Technical University of Denmark for their hospitality. Stimulating and useful discussions with T. C. Bountis, D. W. McLaughlin, and A. C. Scott are gratefully acknowledged.

REFERENCES

1. M. Remoissenet, *Waves Called Solitons* (Springer-Verlag, Berlin, 1994).
2. E. Fermi, J. Pasta, and S. Ulam, in *Collected Papers of Enrico Fermi,* Vol. **2** (Univ. of Chicago Press, Chicago, 1965), p. 978.
3. N. J. Zabusky and M. D. Kruskal, *Phys. Rev. Lett.* **15,** 241 (1965).
4. N.J. Zabusky, *Comp. Phys. Commun.* **5,** 1 (1973).
5. M. Toda, *Phys. Rep.* **18,** 1 (1975).
6. M. A. Collins, *Chem. Phys. Lett.* **77,** 342 (1981).
7. M. Peyrard and M. D. Kruskal, *Physica D* **14,** 88 (1984).
8. A. R. Bishop, J. A. Krumhansl, and S. E. Trullinger, *Physica D* **1,** 1 (1990).
9. A. S. Davydov, *Solitons in Molecular Systems* (Reidel, Dordrecht, 1987).
10. P. L. Christiansen and A.C. Scott (Eds.), *Davydov's Soliton Revisited* (Plenum, New York, 1990).
11. A. C. Scott, *Phys. Rep.* **217,** 1 (1992).
12. O. H. Olsen, P. S. Lomdahl, and W. C. Kerr, *Phys. Lett. A* **136,** 402 (1989).
13. J. Pouget, S. Aubry, A. R. Bishop, and P. S. Lomdahl, *Phys. Rev. B* **39,** 9500 (1989).
14. P. L. Christiansen, P. S. Lomdahl, and V. Muto, *Nonlinearity* **4,** 477 (1990).
15. V. Muto, P. S. Lomdahl, and P. L. Christiansen, *Phys. Rev. A* **42,** 7452 (1990).
16. P. S. Lomdahl, O. H. Olsen, and M. R. Samuelsen, *Phys. Lett. A* **152,** 343 (1991).

17. M. Peyrard and A. R. Bishop, *Phys. Rev. Lett.* **62,** 2755 (1989).
18. M. Peyrard, T. Dauxois, H. Hoyet, and C. R. Willis, *Physica D* **68,** 104 (1993).
19. T. Dauxois, M. Peyrard, nd A. R. Bishop, *Phys. Rev. E.* **47,** R44 (1993).
20. St. Pnevmatikos, A. V. Savin, and A. V. Zolotaryuk, Longitudinal and transverse proton collective dynamics on a two-dimensional multistable substrate, in *Nonlinear Coherent Structures,* Lecture Notes in Physics, Vol. **353,** edited by M. Barthes and J. Léon (Springer-Verlag, New York, 1989), p. 83.
21. A. V. Zolotaryuk and A. V. Savin, *Physica D* **46,** 295 (1990).
22. A. V. Zolotaryuk, St. Pnevmatikos, and A. V. Savin, *Physica D* **51,** 407 (1991).
23. St. Pnevmatikos, A. V. Savin, and A. V. Zolotaryuk, Soliton modelling for the proton transfer in hydrogen-bonded systems, in *Proton Transfer in Hydrogen-Bonded Systems,* edited by T. Bountis (Plenum, New York, 1992), p. 79.
24. J. C. Eilbeck and R. Flesch, *Phys. Lett. A* **149,** 200 (1990).
25. D. B. Duncan, J. C. Eilbeck, H. Feddersen, and J. A. D. Wattis, *Physica D* **68,** 1 (1993).
26. N. Flytzanis, St. Pnevmatikos, and M. Remoissenet, *J. Phys. C: Solid State Phys.* **18,** 4603 (1985).
27. N. Flytzanis, St. Pnevmatikos, and M. Peyrard, *J. Phys. A: Math. Gen.* **22,** 783 (1989).
28. S. Cadet, *Phys. Lett. A* **121,** 77 (1987).
29. J. Frenkel and T. Kontorova, *Phys. Z. Sowjetunion* **13,** 1 (1938).
30. O. M. Braun and Yu. S. Kivshar, *Phys. Rev. B* **44,** 7694 (1991).
31. O. M. Braun, O. A. Chubykalo, Yu. S. Kivshar, and L. Vázquez, *Phys. Rev. B.* **48,** 3734 (1993).
32. S. Yomosa, *Phys. Rev. A* **32,** 1752 (1985).